JOURNAL OF THERMOPHYSICS AND HEAT TRANSFER
Vol. 13, No. 2, April–June 1999

Technical Notes

TECHNICAL NOTES are short manuscripts describing new developments or important results of a preliminary nature. These Notes cannot exceed 6 manuscript pages and 3 figures; a page of text may be substituted for a figure and vice versa. After informal review by the editors, they may be published within a few months of the date of receipt. Style requirements are the same as for regular contributions (see inside back cover).

Depth of Thermal Penetration: Effect of Relaxation and Thermalization

Da Yu Tzou* and Kevin K. S. Chiu†
University of Missouri–Columbia, Columbia, Missouri 65211

Introduction

THERMALIZATION and relaxation are two distinct behaviors in microscale heat transport that become active as the transient time becomes comparable with the thermalization time and/or relaxation time. For continuous media such as pure metals, thermalization and relaxation behaviors could occur in picoseconds.[1–5] For random media with percolating networks, on the other hand, the thermalization and relaxation times could be as long as milliseconds.[6,7] Microstructures dominate the process of heat transport in microscale, as expected. Physically, the thermalization time measures the finite duration in which a second-phase constituent comes to thermal equilibrium with the primary phase. The relaxation time, on the other hand, measures the finite duration in which a sufficient number of collisions among energy carriers take place, leading to an effective heat transport in an engineering sense. The classical model of Fourier diffusion assumes an immediate thermodynamic equilibrium, i.e., a zero thermalization time, and an infinite frequency of collisions among the energy carriers (a zero relaxation time). Resulting from these assumptions, Fourier's law has been found insufficient when used to explain several experimental phenomena in microscale heat transport.[7]

The present work extends the dual-phase lag model,[3–5,7] which describes the interweaving behavior of thermalization and relaxation during the short-time transient, to evaluate the depth of thermal penetration. Through the heat-balance integral approach, the emphasis is placed on the effects of thermal lagging on the time evolution of the thermal penetration depth. Of particular concern is the singular relation between the initial values of the penetration depth and the penetration speed, which does not exist in Fourier diffusion developed at long times.

Depth of Thermal Penetration

The dual-phase lag model captures the microstructural interaction effects in terms of the resulting delayed response in time. In the absence of volumetric heating, the one-dimensional energy equation employing the linearized phase-lag concept is given by[3–5,7]

$$\frac{\partial^2 T}{\partial x^2} + \tau_T \frac{\partial}{\partial t}\left(\frac{\partial^2 T}{\partial x^2}\right) = \frac{1}{\alpha}\frac{\partial T}{\partial t} + \frac{\tau_q}{\alpha}\frac{\partial^2 T}{\partial t^2} \tag{1}$$

The two phase lags, τ_T and τ_q, respectively, measure the finite times required for the thermalization and relaxation processes to complete. To characterize the fundamental behavior in the simplest possible manner, we consider a semi-infinite solid maintained at an initial temperature T_i. A constant temperature T_0 is suddenly imposed at the surface $x = 0$, resulting in a thermal disturbance propagating downstream. In terms of the temperature rise above the boundary temperature T_0, i. e., $T \equiv T - T_0$, the energy equation remains the same while the initial and boundary conditions become

$$T = T_i - T_0, \qquad \frac{\partial T}{\partial t} = 0 \quad \text{as} \quad t = 0 \tag{2}$$

$$T = 0 \quad \text{at} \quad x = 0, \quad T = T_i - T_0 \quad \text{and} \quad \frac{\partial T}{\partial x} = 0 \quad \text{at} \quad x = \delta(t) \tag{3}$$

The depth of thermal penetration, $\delta(t)$, grows with time and is an unknown to be determined.

Following the same procedure as that in the case of Fourier diffusion,[8,9] the integration of Eq. (1) with respect to x in the heat-affected zone from $x = 0$ to $x = \delta(t)$ results in

$$\begin{aligned} &-\frac{\partial T}{\partial x}(x=0,t) + \tau_T\left(-\frac{\partial}{\partial t}\left[\frac{\partial T}{\partial x}(x=0,t)\right]\right. \\ &\left. -\left(\frac{\mathrm{d}\delta}{\mathrm{d}t}\right)\left\{\frac{\partial^2 T}{\partial x^2}[x=\delta(t),t]\right\}\right) \\ &= \frac{1}{\alpha}\left[\frac{\partial}{\partial t}\int_{x=0}^{x=\delta(t)} T(x,t)\,\mathrm{d}x - (T_i - T_0)\frac{\mathrm{d}\delta}{\mathrm{d}t}\right] \\ &+ \frac{\tau_q}{\alpha}\left\{\frac{\partial}{\partial t}\int_{x=0}^{x=\delta(t)} \frac{\partial T}{\partial t}(x,t)\,\mathrm{d}x - \left(\frac{\mathrm{d}\delta}{\mathrm{d}t}\right)\times\frac{\partial T}{\partial t}[x=\delta(t),t]\right\} \end{aligned} \tag{4}$$

Equation (4) is the heat-balance integral accommodating the lagging behavior in microscale heat transfer.

Determination of the depth of thermal penetration, $\delta(t)$, necessitates an approximate distribution of temperature in the heat-affected zone. Assuming a cubic polynomial

$$T(x,t) = (T_i - T_0)\left\{1 - \left[1 - \frac{x}{\delta(t)}\right]^3\right\} \quad \text{for} \quad 0 \le x \le \delta(t) \tag{5}$$

which satisfies all of the boundary conditions in Eq. (3), Eq. (4) reduces to

$$\frac{\mathrm{d}^2\delta}{\mathrm{d}t^2} + \left[\frac{1}{\tau_q} + \left(\frac{12\alpha\tau_T}{\tau_q}\right)\frac{1}{\delta^2}\right]\frac{\mathrm{d}\delta}{\mathrm{d}t} - \left(\frac{12\alpha}{\tau_q}\right)\frac{1}{\delta} = 0 \tag{6}$$

or, in terms of the nondimensional parameters,

$$\theta = \frac{T - T_0}{T_0}, \quad \xi = \frac{x}{\sqrt{\alpha\tau_q}}, \quad \beta = \frac{t}{\tau_q}, \quad \Delta = \frac{\delta}{\sqrt{\alpha\tau_q}}, \quad Z = \frac{\tau_T}{\tau_q} \tag{7}$$

Received May 26, 1998; revision received July 30, 1998; accepted for publication Aug. 31, 1998.

*James C. Dowell Professor, Department of Mechanical and Aerospace Engineering.
†Graduate Research Assistant, Department of Mechanical and Aerospace Engineering.

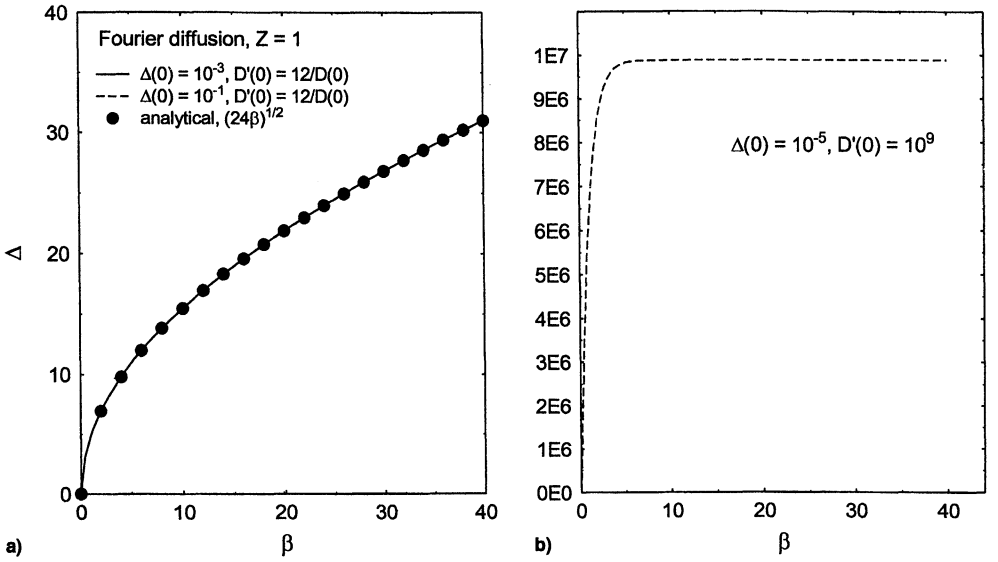

Fig. 1 Case of Fourier diffusion with $Z = 1$: a) comparison of the numerical results and the exact solution for $\Delta(0) = 10^{-1}$ and 10^{-3}, and b) numerical divergence without satisfying the constraint of $\Delta(0) \times [d\Delta/d\beta(0)] = 12$.

Equation (6) gives

$$\frac{d^2\Delta}{d\beta^2} + \left(1 + \frac{12Z}{\Delta^2}\right)\frac{d\Delta}{d\beta} - \frac{12}{\Delta} = 0 \tag{8}$$

Equation (8) displays a second-order nonlinear ordinary differential equation, which clearly shows that the ratio $Z\ (=\tau_T/\tau_q)$ is the only parameter that dictates the time evolution of the thermal penetration depth. The relations between the ratio Z and the various microscopic structural parameters were summarized by Tzou.[7]

The initial thermal penetration speed ($d\Delta/d\beta$ as $\beta = 0$) necessitates an analytical study because the initial thermal penetration depth, $\Delta = 0$ as $\beta = 0$, introduces a singularity to Eq. (8). For this purpose, we introduce

$$\Delta \times \left(\frac{d\Delta}{d\beta}\right) = F(\Delta) \tag{9}$$

Substituting Eq. (9) into Eq. (8), it results in a first-order differential equation for $F(\Delta)$:

$$(\Delta \times F)\frac{dF}{d\Delta} - F^2 + (\Delta^2 + 12Z)F - 12\Delta^2 = 0 \tag{10}$$

In passing to the limit of $\Delta \to 0$ as $\beta \to 0$, Eq. (17) gives $F \equiv \Delta \times (d\Delta/d\beta) = 12Z$. The two initial conditions required for solving Eq. (8) numerically, therefore, are more precisely expressed as

$$\Delta \to 0 \quad \text{and} \quad \frac{d\Delta}{d\beta} \to \frac{12Z}{\Delta} \quad \text{as} \quad \beta = 0 \tag{11}$$

A small value for $\Delta(0)$ can be chosen to approximate the initial penetration depth. The initial penetration speed, however, needs to be calculated according to Eq. (11), to ensure the numerical convergence. The case of Fourier diffusion is retrieved as $Z = 1$.[3-5,7] Equation (11) can be solved exactly in this case

$$\Delta \times \left(\frac{d\Delta}{d\beta}\right) = 12 \quad \text{or} \quad \Delta = \sqrt{24\beta} \quad \text{(Fourier diffusion)} \tag{12}$$

which is a familiar result.[10]

Numerical Results

The fourth-order Runge-Kutta method with adaptive step-size control[11] is used to compute the depth of thermal penetration according to Eq. (8). The fractional accuracy is set to be 10^{-10}. For the case of Fourier diffusion, $Z = 1$, Fig. 1a compares the numerical solution to Eq. (8) with the exact solution shown in Eq. (12). As long as the relation shown by Eq. (11) is satisfied, the selection of the initial penetration depth is somewhat forgiving. A value of $\Delta(0) = 10^{-1}$ can give as accurate a result as $\Delta(0) = 10^{-3}$. Figure 1b explicitly demonstrates the importance of Eq. (11). Numerical divergence results if a small value of the initial penetration depth [$\Delta(0) = 10^{-5}$] and a large value of the initial penetration speed [$\Delta'(0) = 10^9$] are arbitrarily chosen without satisfying Eq. (11), although these values are closer to the real situations. Figure 2a displays the time history of penetration depth for $Z = 1$ (Fourier diffusion), 10, and 50, with $\Delta(0) = 10^{-3}$ and $d\Delta/d\beta(0) = 12{,}000Z$ in accordance with Eq. (11). At short times, the depth of thermal penetration increases with the value of Z. As time lengthens, the transient curves crosses the curve of Fourier diffusion ($Z = 1$), and then merge from below. Fourier diffusion results in a straight line with a slope being one-half (1/2) on a logarithmic scale, as shown in Fig. 2b. In the presence of thermal lagging ($Z > 1$) during the short-time transient, however, the response curves for the depth of thermal penetration are nonlinear, with a slope being less than one-half. The slope of the response curves seems to be close to one-half at short times ($\beta < 0.5$), but the difference between the results of thermal lagging and Fourier diffusion is significant in this domain. Temperature distributions within the heat affected zone are shown in Fig. 3 for $\beta = 2$ (Fig. 3a) and $\beta = 10$ (Fig. 3b). The analytical solutions employing the Riemann-sum approximation for the Laplace inversion[3-5,7] are included for comparison. The difference between the heat-balance integral and the Riemann-sum approximation is less than 10% in all cases, with the near-surface temperature at $\xi = 0$ being particularly accurate.

Thermal lagging is a special behavior that exists for response time comparable to the thermalization time (τ_T) and the relaxation time (τ_q). Under constant thermal properties, this can be demonstrated by casting Eq. (1) into the following form:

$$\frac{\partial^2 T}{\partial x^2} + \frac{\partial}{\partial(t/\tau_T)}\frac{\partial^2 T}{\partial x^2} = \frac{1}{\alpha}\frac{\partial T}{\partial t} + \frac{1}{\alpha}\frac{\partial}{\partial(t/\tau_q)}\frac{\partial T}{\partial t} \tag{13}$$

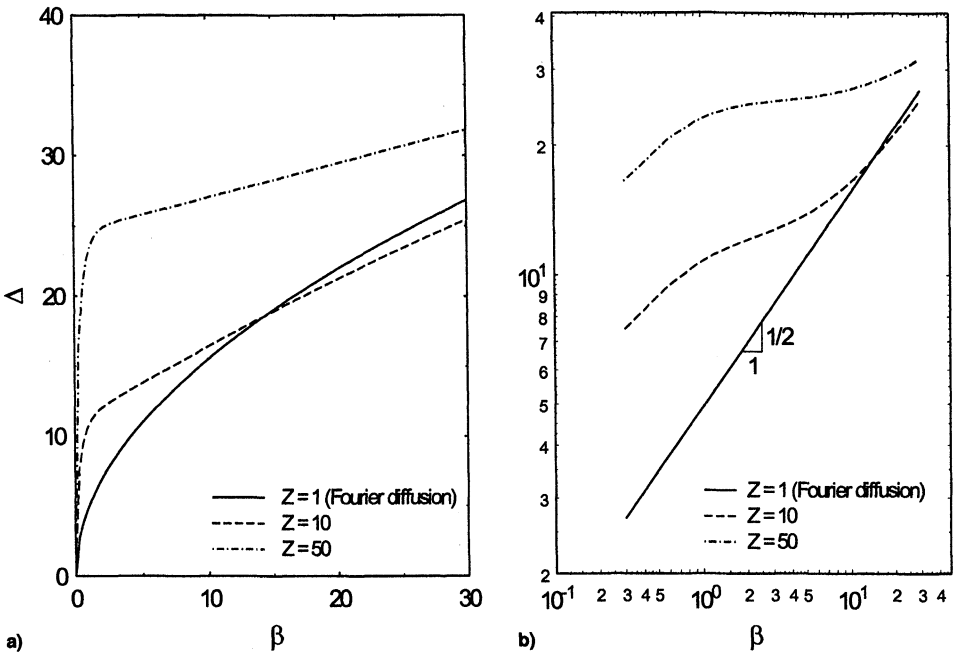

Fig. 2 a) Depth of thermal penetration (Δ) varying as a function of time (β) at Z = 1, 10, and 50, and b) the logarithmic representation of Fig. 2a.

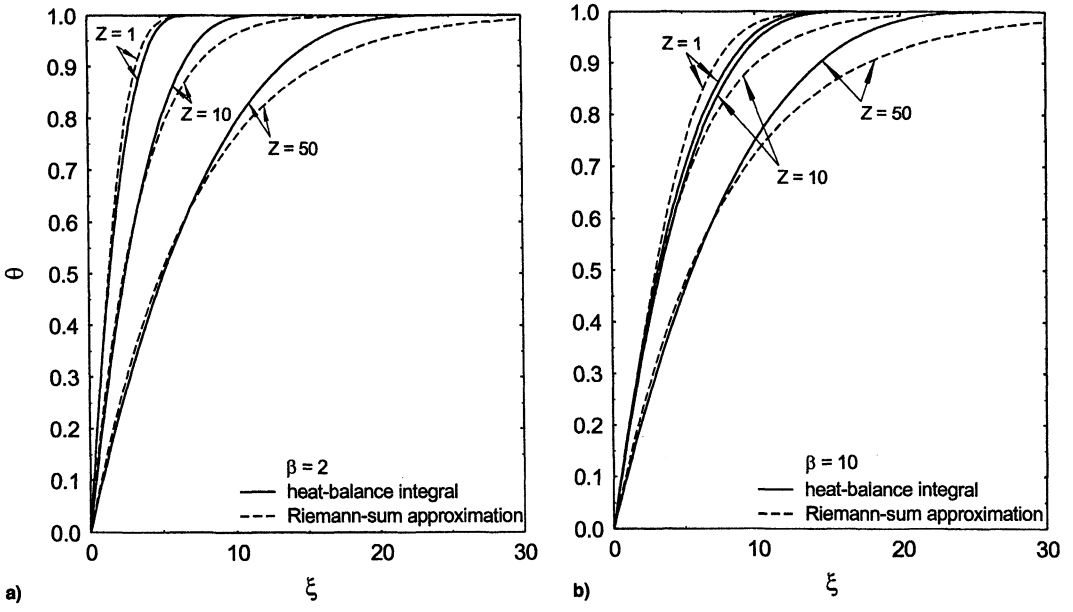

Fig. 3 Temperature distributions in the heat-affected zone and comparison with the results of Riemann-sum approximation at β = a) 2 and b) 10. Z = 1, 10, and 50.

As the transient time lengthens, the ratios of (t/τ_T) and (t/τ_q) increase, resulting in gradually diminishing effects from thermalization [the second term on the left side of Eq. (13)], and relaxation [the second term on the right side of Eq. (13)]. The classical effect of Fourier diffusion [the second term on the right side of Eq. (13)] remains in this process, supporting that the Fourier response will be retrieved priori to the steady-state response as illustrated in Fig. 2.

The thermal-lagging model retrieves the microscopic phonon–electron-interaction model and the phonon-interaction model in limiting cases.[3–5,7] Under constant thermal properties, for example, the parameter Z characterizing the lagging behavior relates to the following microstructural parameters:

$$Z = \begin{cases} 1 + (C_l/C_e), & \text{phonon–electron interaction model} \\ \frac{9}{5}(\tau_N/\tau_R), & \text{phonon scattering model} \end{cases} \quad (14)$$

where C_e and C_l are volumetric heat capacities of the electron gas and the metal lattice, respectively, τ_N is the relaxation time in the normal process of phonon collision; and τ_R is relaxation time in the umklapp process of phonon collision. When the value of Z varies in Figs. 2 and 3, it can be interpreted as the variations of the heat-capacity ratio (in phonon–electron interaction) and the relaxation-time ratio (in phonon scattering) shown in Eq. (14).

Conclusions

The concept of heat-balance integral, and the resulting depth of thermal penetration, has been extended to accommodate the effects of thermalization and relaxation during the short-time transient. The relation between the initial penetration depth and the initial penetration speed has been determined analytically, which has proven essential for achieving numerical conver-

gence. This situation has been ignored in the past because the equation governing the thermal penetration depth in the case of Fourier diffusion is directly integrable.

The two phase lags, τ_T and τ_q, and, hence, the ratio Z, may be strong functions of temperature, especially for τ_q. With the fundamental framework for the heat balance integral laid down in this work, extensions to accommodate the temperatue-dependent phase lags can readily be made. This will be left for a future communication.

References

[1]Qiu, T. Q., and Tien, C. L., "Short-Pulse Laser Heating on Metals," *International Journal of Heat and Mass Transfer*, Vol. 35, 1992, pp. 719–726.

[2]Qiu, T. Q., and Tien, C. L., "Heat Transfer Mechanisms During Short-Pulse Laser Heating of Metals," *Journal of Heat Transfer*, Vol. 115, 1993, pp. 835–841.

[3]Tzou, D. Y., "A Unified Field Approach for Heat Conduction from Macro- to Microscales," *Journal of Heat Transfer*, Vol. 117, 1995, pp. 8–16.

[4]Tzou, D. Y., "The Generalized Lagging Response in Small-Scale and High-Rate Heating," *International Journal of Heat and Mass Transfer*, Vol. 38, 1995, pp. 3231–3240.

[5]Tzou, D. Y., "Experimental Support for the Lagging Response in Heat Propagation," *Journal of Thermophysics and Heat Transfer*, Vol. 9, 1995, pp. 686–693.

[6]Fournier, D., and Boccara, A. C., "Heterogeneous Media and Rough Surfaces: A Fractal Approach for Heat Diffusion Studies," *Physica (A)*, Vol. 157, 1989, pp. 587–592.

[7]Tzou, D. Y., *Macro- to Microscale Heat Transfer: The Lagging Behavior*, Taylor and Francis, Washington, DC, 1997.

[8]Goodman, T. R., "The Heat Balance Integral: Further Consideration and Refinements," *Journal of Heat Transfer*, Vol. 32, 1961, pp. 83–86.

[9]Goodman, T. R., "Application of Integral Methods to Transient Nonlinear Heat Transfer," *Advances in Heat Transfer*, Vol. 1, 1964, pp. 55–122.

[10]Eckert, E. R. G., and Drake, R. M., Jr., *Analysis of Heat and Mass Transfer*, McGraw–Hill, New York, 1972.

[11]Press, W. H., Teukolsky, S. A., Vetterling, W. T., and Flannery, B. P., *Numerical Recipes in FORTRAN*, Cambridge Univ. Press, New York, 1992, pp. 708–716.

Analytical Comparison of Constant Area, Adiabatic Tip, Standard Fins, and Heat Pipe Fins

W. Jerry Bowman,* J. Kirk Storey,†
and Kenth I. Svensson†
Brigham Young University, Provo, Utah 84602

Introduction

ELECTRONIC equipment, as well as many other applications, need to be kept within certain temperature limits to function properly and safely. Increasing the surface area, and thus, the heat transfer, using fins attached to the high-temperature areas of the devices is a common solution.

To improve heat dissipation without using larger surface areas, fin efficiency must be increased. One way to improve fin efficiency is through higher thermal conductivity fin materials. Heat pipes have effective thermal conductivities that are one to two orders of magnitude higher than solid fins, and can be considered as an effective substitution for solid fins. Another benefit of heat pipes is their inherent fast thermal response time. Peterson[1] shows an example where 20 W of thermal energy is transferred 0.5 m in a device 1.27 cm in diameter. A solid aluminum fin, a solid copper fin, and a heat pipe were compared using Fourier's law. A copper–water heat pipe with a screen wick was used. The temperature differences along the fins were 460, 206, and 6°C, respectively, which demonstrates the much higher effective thermal conductivity in heat pipes. The copper–water heat pipe was also 76 and 93% lighter than the aluminum and copper fins, respectively.

Zhao and Avedisian[2] researched the concept of adding fins to a copper–water heat pipe to increase the heat transfer. Their study consisted of a fixed fin pitch and a fixed fin shape in a forced convection environment. They achieved a heat flux of 80 W/cm^2 and a total power of 800 W for the longest finned heat pipe tested. By comparison, a finned copper rod of the same length only attained 30 W/cm^2 and a total power of 300 W. Particularly interesting data resulted from their tests of shorter heat pipes. In these cases, the solid copper rod performed better than the heat pipe, suggesting that heat pipes may not always be beneficial. The longer the test specimen, the more the heat pipe outperformed the copper rod.

Another study shows a brass fin made from a planar heat pipe with water as the working fluid.[3] The fin was mounted horizontally. They reported a 22% improvement in fin efficiency for this arrangement. This is a significant improvement over standard fins.

The purpose of this study is to derive an expression for a constant area, adiabatic end condition, heat pipe fin efficiency. This will be used to compare the performance of a heat pipe fin with a standard fin.

Heat Pipe Fin Efficiency

Figure 1 illustrates the heat pipe fin being considered. Neglecting radiation, assuming steady state, and assuming that the temperature varies only in the x direction, conservation of energy applied to a differential element of the wall is

$$k(A - A_v)\frac{\partial^2 T}{\partial x^2} - h_0 P_0 (T - T_\infty) - h_i P_i (T - T_v) = 0 \quad (1)$$

where k is thermal conductivity of the heat pipe wall, A is the cross-sectional area of the heat pipe (wall plus vapor space), A_v is the cross-sectional area of the vapor space, T is the wall temperature, h_0 is the convection heat transfer coefficient on the outside of the heat pipe, P_0 is the outside perimeter of the heat pipe, T_∞ is the temperature surrounding the heat pipe, h_i is the convection heat transfer coefficient on the inside of the

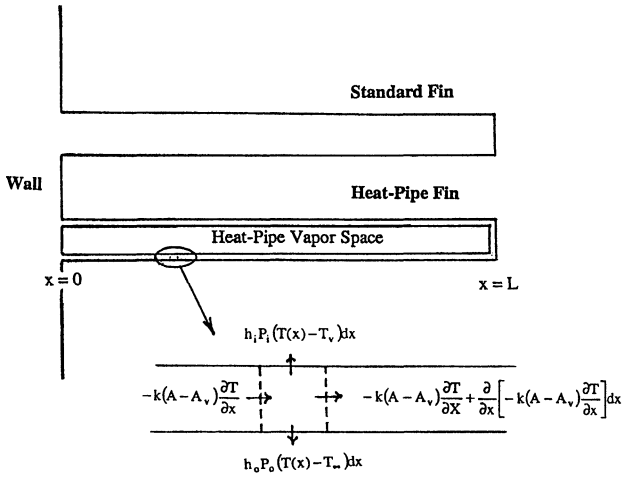

Fig. 1 Heat pipe fin control volume.

Received Aug. 21, 1998; revision received Nov. 9, 1998; accepted for publication Nov. 9, 1998.

*Associate Professor, Department of Mechanical Engineering.
†Research Assistant, Department of Mechanical Engineering.